Supplementary Information for: "Prediction and Observation of Intermodulation Sidebands from Anharmonic Phonons in NaBr"

Y. Shen,[1,*] C. N. Saunders,[1] C. M. Bernal,[1] D. L. Abernathy,[2] T. J. Williams,[2] M. E. Manley,[3] and B. Fultz[1,†]

[1] *Department of Applied Physics and Materials Science, California Institute of Technology, Pasadena, California 91125, USA*

[2] *Neutron Scattering Division, Oak Ridge National Laboratory, Oak Ridge, Tennessee 37831, USA*

[3] *Material Science and Technology Division, Oak Ridge National Laboratory, Oak Ridge, Tennessee 37831, USA*

(Dated: March 14, 2021)

CLASSICAL ANALYSIS

Consider the original Heisenberg-Langevin equations (Eq. 6-7 in the main text):

$$\dot{\hat{a}} = -\mathrm{i}\omega_1 \hat{a} - \mathrm{i}\eta\hat{a}\left(\hat{b}^\dagger + \hat{b}\right) - \frac{\gamma_1}{2}\hat{a} - \sqrt{\gamma_1}\hat{\xi}_1 \ , \tag{S1}$$

$$\dot{\hat{b}} = -\mathrm{i}\omega_2 \hat{b} - \mathrm{i}\frac{\eta}{2}\left(\hat{a}^\dagger\hat{a} + \hat{a}\hat{a}^\dagger\right) - \frac{\gamma_2}{2}\hat{b} - \sqrt{\gamma_2}\hat{\xi}_2 \ . \tag{S2}$$

Following the method in Ref. [1], we can replace the phonon amplitudes with a Fourier decomposition of sidebands as

$$\hat{a} \longrightarrow \alpha = \sum_j A_j e^{-\mathrm{i}\omega_{a,j}t}, \qquad b \longrightarrow B_0 e^{-\mathrm{i}\omega_2 t} \ , \tag{S3}$$

where j is the sideband order. Substituting these into Eq. S1

$$\sum_j -\mathrm{i}\omega_{a,j}A_j e^{-\mathrm{i}\omega_{a,j}t} = -\left(\mathrm{i}\omega_1 + \frac{\gamma_1}{2}\right)\sum_j A_j e^{-\mathrm{i}\omega_{a,j}t} - \mathrm{i}\eta B_0 \sum_j A_j\left(e^{-\mathrm{i}(\omega_{a,j}+\omega_2)t} + e^{-\mathrm{i}(\omega_{a,j}-\omega_2)t}\right) \ . \tag{S4}$$

Comparing the two sides of Eq. S4, we find the intermodulation frequencies

$$\begin{aligned} \text{First order}: &\ j=1,\ \omega_{a,1} = \omega_1; \\ \text{Second order}: &\ j=2,\ \omega_{a,2} = \omega_1 \pm \omega_2; \\ \text{Third order}: &\ j=3,\ \omega_{a,3} = \omega_{a,2} \pm \omega_2 = \omega_1 \pm 2\omega_2; \\ &\ \ldots \end{aligned} \tag{S5}$$

SOLVING THE QUANTUM LANGEVIN EQUATIONS

The Heisenberg-Langevin equations in the main text (Eq. 7) can be solved by Fourier transformation.For an operator in the time domain $\hat{O}(t)$, we use an operator in the frequency domain, $\hat{O}[\omega]$

$$\hat{O}[\omega] = \frac{1}{\sqrt{2\pi}}\int_{-\infty}^{+\infty} \mathrm{d}t e^{\mathrm{i}\omega t}\hat{O}(t) \ , \tag{S6}$$

$$\hat{O}^\dagger[\omega] = \frac{1}{\sqrt{2\pi}}\int_{-\infty}^{+\infty} \mathrm{d}t e^{\mathrm{i}\omega t}\hat{O}^\dagger(t) \ . \tag{S7}$$

This procedure gives the following Fourier transformed equations

$$(-\mathrm{i}\omega + \frac{\gamma_1}{2})\hat{c}[\omega] = -\mathrm{i}g\left(\hat{b}^\dagger[\omega] + \hat{b}[\omega]\right) - \sqrt{\gamma_1}\hat{\xi}_1[\omega]\ , \tag{S8}$$

$$(-\mathrm{i}\omega + \frac{\gamma_1}{2})\hat{c}^\dagger[\omega] = \mathrm{i}g\left(\hat{b}^\dagger[\omega] + \hat{b}[\omega]\right) - \sqrt{\gamma_1}\hat{\xi_1}^\dagger[\omega]\ , \tag{S9}$$

$$\left[-\mathrm{i}(\omega-\omega_2) + \frac{\gamma_2}{2}\right]\hat{b}[\omega] = -\mathrm{i}g\left(\hat{c}^\dagger[\omega] + \hat{c}[\omega]\right) - \sqrt{\gamma_2}\hat{\xi}_2[\omega]\ , \tag{S10}$$

$$\left[-\mathrm{i}(\omega+\omega_2) + \frac{\gamma_2}{2}\right]\hat{b}^\dagger[\omega] = \mathrm{i}g\left(\hat{c}^\dagger[\omega] + \hat{c}[\omega]\right) - \sqrt{\gamma_2}\hat{\xi}_2^\dagger[\omega]\ . \tag{S11}$$

Solutions forf $\hat{c}$ and $\hat{c}^\dagger$ are

$$\hat{c}[\omega] = \chi_c^2\chi_b\bar{\chi}_b\left\{-\sqrt{\gamma_1}\left[\left(\chi_c^{-1}\chi_b^{-1}\bar{\chi}_b^{-1} + 2\mathrm{i}\omega_2 g^2\right)\hat{\xi}_1 + 2\mathrm{i}\omega_2 g^2\hat{\xi}_1^\dagger\right] + \mathrm{i}g\sqrt{\gamma_2}\chi_c^{-1}\left(\bar{\chi}_b^{-1}\hat{\xi}_2 + \chi_b^{-1}\hat{\xi}_2^\dagger\right)\right\}\ , \tag{S12}$$

$$\hat{c}^\dagger[\omega] = \chi_c^2\chi_b\bar{\chi}_b\left\{-\sqrt{\gamma_1}\left[-2\mathrm{i}\omega_2 g^2\hat{\xi}_1 + \left(\chi_c^{-1}\chi_b^{-1}\bar{\chi}_b^{-1} - 2\mathrm{i}\omega_2 g^2\right)\hat{\xi}_1^\dagger\right] - \mathrm{i}g\sqrt{\gamma_2}\chi_c^{-1}\left(\bar{\chi}_b^{-1}\hat{\xi}_2 + \chi_b^{-1}\hat{\xi}_2^\dagger\right)\right\}\ , \tag{S13}$$

where the bare response functions are

$$\chi_c^{-1} = -\mathrm{i}\omega + \frac{\gamma_1}{2}\ , \tag{S14}$$

$$\chi_b^{-1} = -\mathrm{i}(\omega-\omega_2) + \frac{\gamma_2}{2}\ , \tag{S15}$$

$$\bar{\chi}_b^{-1} = -\mathrm{i}(\omega+\omega_2) + \frac{\gamma_2}{2}\ . \tag{S16}$$

Transforming back to the original operators $\hat{a}$ ($\hat{a}^\dagger$), the position operator is obtained

$$\hat{x} = x_{\mathrm{zpf}}\left(\hat{a} + \hat{a}^\dagger\right) = x_{\mathrm{zpf}}\left[(\alpha + \hat{c})\,e^{-\mathrm{i}\omega_1 t} + \left(\alpha + \hat{c}^\dagger\right)e^{\mathrm{i}\omega_1 t}\right]\ , \tag{S17}$$

with $x_{\mathrm{zpf}} = \sqrt{\frac{\hbar}{2m\omega_1}}$ as the amplitude of zero point fluctuations. Correspondingly

$$x[\omega] = x_{\mathrm{zpf}}\left(c[\omega-\omega_1] + c^\dagger[\omega+\omega_1] + \alpha\delta[\omega-\omega_1] + \alpha\delta[\omega+\omega_1]\right)\ . \tag{S18}$$

Neglecting the unimportant terms of single δ-functions, the displacement power spectral density, $S_{xx}[\omega]$, can be obtained by

$$\begin{aligned} S_{xx}[\omega] &= \int_{-\infty}^{+\infty}\langle\hat{x}[\omega]\hat{x}[\omega']\rangle\,\mathrm{d}\omega' \\ &= \frac{\hbar}{2m\omega_1}\int_{-\infty}^{+\infty}\left\langle\left(c[\omega-\omega_1] + c^\dagger[\omega+\omega_1]\right)\left(c[\omega'-\omega_1] + c^\dagger[\omega'+\omega_1]\right)\right\rangle\mathrm{d}\omega' \\ &= \frac{\hbar}{2m\omega_1}\left(\int_{-\infty}^{+\infty}\langle c[\omega-\omega_1]c[\omega'-\omega_1]\rangle\,\mathrm{d}\omega' + \int_{-\infty}^{+\infty}\left\langle c[\omega-\omega_1]c^\dagger[\omega'+\omega_1]\right\rangle\mathrm{d}\omega'\right. \\ &\qquad\left. + \int_{-\infty}^{+\infty}\left\langle c^\dagger[\omega+\omega_1]c[\omega'-\omega_1]\right\rangle\mathrm{d}\omega' + \int_{-\infty}^{+\infty}\left\langle c^\dagger[\omega+\omega_1]c^\dagger[\omega'+\omega_1]\right\rangle\mathrm{d}\omega'\right) \end{aligned} \tag{S19}$$

In the frequency domain, the input noise operators satisfy the relations of

$$\left\langle\hat{\xi}_{1,2}[\omega_1]\hat{\xi}_{1,2}^\dagger[\omega_2]\right\rangle = (n_{1,2}+1)\delta[\omega_1+\omega_2]\ , \tag{S20}$$

$$\left\langle\hat{\xi}_{1,2}^\dagger[\omega_1]\hat{\xi}_{1,2}[\omega_2]\right\rangle = n_{1,2}\delta[\omega_1+\omega_2]\ . \tag{S21}$$

Employing these relations, every term in Eq. S19 can be calculated

$$\begin{aligned}
&\int_{-\infty}^{+\infty} \langle c[\omega-\omega_1]c[\omega'-\omega_1]\rangle \,\mathrm{d}\omega' \\
=&\,\gamma_1 \left|\chi_{a,-}^2\chi_{b,-}\bar{\chi}_{b,-}\right|^2 \left(2\mathrm{i}\omega_2 g^2\right)\left[\left(\chi_{a,-}^{-1}\chi_{b,-}^{-1}\bar{\chi}_{b,-}^{-1}+2\mathrm{i}\omega_2 g^2\right)(n_1+1)+\left(\chi_{a,-}^{*-1}\chi_{b,-}^{*-1}\bar{\chi}_{b,-}^{*-1}+2\mathrm{i}\omega_2 g^2\right)n_1\right] \\
&-g^2\gamma_2 \left|\chi_{a,-}\chi_{b,-}\bar{\chi}_{b,-}\right|^2\left(\left|\bar{\chi}_{b,-}^{-1}\right|^2(n_2+1)+\left|\chi_{b,-}^{-1}\right|^2 n_2\right)\,,
\end{aligned}\tag{S22}$$

$$\begin{aligned}
&\int_{-\infty}^{+\infty} \left\langle c[\omega-\omega_1]c^\dagger[\omega'+\omega_1]\right\rangle \,\mathrm{d}\omega' \\
=&\,\gamma_1 \left|\chi_{a,-}^2\chi_{b,-}\bar{\chi}_{b,-}\right|^2 \left[\left|\chi_{a,-}^{-1}\chi_{b,-}^{-1}\bar{\chi}_{b,-}^{-1}+2\mathrm{i}\omega_2 g^2\right|^2(n_1+1)+4\omega_2^2 g^4 n_1\right] \\
&+g^2\gamma_2 \left|\chi_{a,-}\chi_{b,-}\bar{\chi}_{b,-}\right|^2\left(\left|\bar{\chi}_{b,-}^{-1}\right|^2(n_2+1)+\left|\chi_{b,-}^{-1}\right|^2 n_2\right)\,,
\end{aligned}\tag{S23}$$

$$\begin{aligned}
&\int_{-\infty}^{+\infty} \left\langle c^\dagger[\omega+\omega_1]c[\omega'-\omega_1]\right\rangle \,\mathrm{d}\omega' \\
=&\,\gamma_1 \left|\chi_{a,+}^2\chi_{b,+}\bar{\chi}_{b,+}\right|^2 \left[4\omega_2^2 g^4(n_1+1)+\left|\chi_{a,+}^{-1}\chi_{b,+}^{-1}\bar{\chi}_{b,+}^{-1}-2\mathrm{i}\omega_2 g^2\right|^2 n_1\right] \\
&+g^2\gamma_2 \left|\chi_{a,+}\chi_{b,+}\bar{\chi}_{b,+}\right|^2\left(\left|\bar{\chi}_{b,+}^{-1}\right|^2(n_2+1)+\left|\chi_{b,+}^{-1}\right|^2 n_2\right)\,,
\end{aligned}\tag{S24}$$

$$\begin{aligned}
&\int_{-\infty}^{+\infty} \left\langle c^\dagger[\omega+\omega_1]c^\dagger[\omega'+\omega_1]\right\rangle \,\mathrm{d}\omega' \\
=&\,\gamma_1 \left|\chi_{a,+}^2\chi_{b,+}\bar{\chi}_{b,+}\right|^2 \left(-2\mathrm{i}\omega_2 g^2\right)\left[\left(\chi_{a,+}^{*-1}\chi_{b,+}^{*-1}\bar{\chi}_{b,+}^{*-1}-2\mathrm{i}\omega_2 g^2\right)(n_1+1)+\left(\chi_{a,+}^{-1}\chi_{b,+}^{-1}\bar{\chi}_{b,+}^{-1}-2\mathrm{i}\omega_2 g^2\right)n_1\right] \\
&-g^2\gamma_2 \left|\chi_{a,+}\chi_{b,+}\bar{\chi}_{b,+}\right|^2\left(\left|\bar{\chi}_{b,+}^{-1}\right|^2(n_2+1)+\left|\chi_{b,+}^{-1}\right|^2 n_2\right)\,,
\end{aligned}\tag{S25}$$

where the response functions are

$$\chi_{a,\pm}^{-1} = -\mathrm{i}(\omega\pm\omega_1)+\frac{\gamma_1}{2}\,,\tag{S26}$$

$$\chi_{b,\pm}^{-1} = -\mathrm{i}(\omega\pm\omega_1-\omega_2)+\frac{\gamma_2}{2}\,,\tag{S27}$$

$$\bar{\chi}_{b,\pm}^{-1} = -\mathrm{i}(\omega\pm\omega_1+\omega_2)+\frac{\gamma_2}{2}\,.\tag{S28}$$

Taking $\int_{-\infty}^{+\infty} \langle c[\omega-\omega_1]c[\omega'-\omega_1]\rangle \,\mathrm{d}\omega'$ as an example, Eq. S22 can be derived as follows:

$$\begin{aligned}
&\int_{-\infty}^{+\infty} \langle c[\omega-\omega_1]c[\omega'-\omega_1]\rangle \,\mathrm{d}\omega' \\
=&\int_{-\infty}^{+\infty} \mathrm{d}\omega' \chi_c^2[\omega-\omega_1]\chi_b[\omega-\omega_1]\bar{\chi}_b[\omega-\omega_1]\chi_c^2[\omega'-\omega_1]\chi_b[\omega'-\omega_1]\bar{\chi}_b[\omega'-\omega_1] \\
&\Big\{\gamma_1\Big[\left(\chi_c^{-1}[\omega-\omega_1]\chi_b^{-1}[\omega-\omega_1]\bar{\chi}_b^{-1}[\omega-\omega_1]+2\mathrm{i}\omega_2 g^2\right)\left(2\mathrm{i}\omega_2 g^2\right)\left\langle \hat{\xi}_1[\omega-\omega_1]\hat{\xi}_1^\dagger[\omega'-\omega_1]\right\rangle \\
&\qquad+\left(\chi_c^{-1}[\omega'-\omega_1]\chi_b^{-1}[\omega'-\omega_1]\bar{\chi}_b^{-1}[\omega'-\omega_1]+2\mathrm{i}\omega_2 g^2\right)\left(2\mathrm{i}\omega_2 g^2\right)\left\langle \hat{\xi}_1^\dagger[\omega-\omega_1]\hat{\xi}_1[\omega'-\omega_1]\right\rangle\Big] \\
&\quad-g^2\gamma_2\chi_c^{-1}[\omega-\omega_1]\chi_c^{-1}[\omega'-\omega_1] \\
&\quad\left(\bar{\chi}_b^{-1}[\omega-\omega_1]\chi_b^{-1}[\omega'-\omega_1]\left\langle \hat{\xi}_2[\omega-\omega_1]\hat{\xi}_2^\dagger[\omega'-\omega_1]\right\rangle+\chi_b^{-1}[\omega-\omega_1]\bar{\chi}_b^{-1}[\omega'-\omega_1]\left\langle \hat{\xi}_2^\dagger[\omega-\omega_1]\hat{\xi}_2[\omega'-\omega_1]\right\rangle\right)\Big\} \\
=&\int_{-\infty}^{+\infty} \mathrm{d}\omega' \chi_c^2[\omega-\omega_1]\chi_b[\omega-\omega_1]\bar{\chi}_b[\omega-\omega_1]\chi_c^2[\omega'-\omega_1]\chi_b[\omega'-\omega_1]\bar{\chi}_b[\omega'-\omega_1]
\end{aligned}$$

$$\Bigg\{\gamma_1\Big[\left(\chi_c^{-1}[\omega-\omega_1]\chi_b^{-1}[\omega-\omega_1]\bar{\chi}_b^{-1}[\omega-\omega_1]+2\mathrm{i}\omega_2 g^2\right)\left(2\mathrm{i}\omega_2 g^2\right)(n_1+1)\,\delta\left[\omega'-(2\omega_1-\omega)\right]$$
$$+\left(\chi_c^{-1}[\omega'-\omega_1]\chi_b^{-1}[\omega'-\omega_1]\bar{\chi}_b^{-1}[\omega'-\omega_1]+2\mathrm{i}\omega_2 g^2\right)\left(2\mathrm{i}\omega_2 g^2\right)n_1\delta\left[\omega'-(2\omega_1-\omega)\right]\Big]$$
$$-g^2\gamma_2\chi_c^{-1}[\omega-\omega_1]\chi_c^{-1}[\omega'-\omega_1]$$
$$\left(\bar{\chi}_b^{-1}[\omega-\omega_1]\chi_b^{-1}[\omega'-\omega_1]\,(n_2+1)\,\delta\left[\omega'-(2\omega_1-\omega)\right]+\chi_b^{-1}[\omega-\omega_1]\bar{\chi}_b^{-1}[\omega'-\omega_1]n_2\delta\left[\omega'-(2\omega_1-\omega)\right]\right)\Bigg\}$$
$$=\chi_c^2[\omega-\omega_1]\chi_b[\omega-\omega_1]\bar{\chi}_b[\omega-\omega_1]\chi_c^2[\omega_1-\omega]\chi_b[\omega_1-\omega]\bar{\chi}_b[\omega_1-\omega]$$
$$\Bigg\{\gamma_1\Big[\left(\chi_c^{-1}[\omega-\omega_1]\chi_b^{-1}[\omega-\omega_1]\bar{\chi}_b^{-1}[\omega-\omega_1]+2\mathrm{i}\omega_2 g^2\right)\left(2\mathrm{i}\omega_2 g^2\right)(n_1+1)$$
$$+\left(\chi_c^{-1}[\omega_1-\omega]\chi_b^{-1}[\omega_1-\omega]\bar{\chi}_b^{-1}[\omega_1-\omega]+2\mathrm{i}\omega_2 g^2\right)\left(2\mathrm{i}\omega_2 g^2\right)n_1\Big]$$
$$-g^2\gamma_2\chi_c^{-1}[\omega-\omega_1]\chi_c^{-1}[\omega_1-\omega]\left(\bar{\chi}_b^{-1}[\omega-\omega_1]\chi_b^{-1}[\omega_1-\omega]\,(n_2+1)+\chi_b^{-1}[\omega-\omega_1]\bar{\chi}_b^{-1}[\omega_1-\omega]n_2\right)\Bigg\}$$
$$=\gamma_1\left|\chi_{a,-}^2\chi_{b,-}\bar{\chi}_{b,-}\right|^2\left(2\mathrm{i}\omega_2 g^2\right)\left[\left(\chi_{a,-}^{-1}\chi_{b,-}^{-1}\bar{\chi}_{b,-}^{-1}+2\mathrm{i}\omega_2 g^2\right)(n_1+1)+\left(\chi_{a,-}^{*-1}\chi_{b,-}^{*-1}\bar{\chi}_{b,-}^{*-1}+2\mathrm{i}\omega_2 g^2\right)n_1\right]$$
$$-g^2\gamma_2\left|\chi_{a,-}\chi_{b,-}\bar{\chi}_{b,-}\right|^2\left(\left|\bar{\chi}_{b,-}^{-1}\right|^2(n_2+1)+\left|\chi_{b,-}^{-1}\right|^2 n_2\right)\ , \tag{S29}$$

Finally, the displacement power spectral density is

$$S_{xx}[\omega]=\frac{\hbar\gamma_1}{2m\omega_1}\left|\chi_{a,-}^2\chi_{b,-}\bar{\chi}_{b,-}\right|^2\Bigg\{\left|\chi_{a,-}^{-2}\chi_{b,-}^{-1}\bar{\chi}_{b,-}^{-1}+2\mathrm{i}\omega_2 g^2\right|^2(n_1+1)+4\omega_2^2 g^4 n_1$$
$$+2\mathrm{i}\omega_2 g^2\left[\left(\chi_{a,-}^{-1}\chi_{b,-}^{-1}\bar{\chi}_{b,-}^{-1}+2\mathrm{i}\omega_2 g^2\right)(n_1+1)+\left(\chi_{a,-}^{*-1}\chi_{b,-}^{*-1}\bar{\chi}_{b,-}^{*-1}+2\mathrm{i}\omega_2 g^2\right)n_1\right]\Bigg\}$$
$$+\frac{\hbar\gamma_1}{2m\omega_1}\left|\chi_{a,+}^2\chi_{b,+}\bar{\chi}_{b,+}\right|^2\Bigg\{\left|\chi_{a,+}^{-2}\chi_{b,+}^{-1}\bar{\chi}_{b,+}^{-1}-2\mathrm{i}\omega_2 g^2\right|^2 n_1+4\omega_2^2 g^4(n_1+1)$$
$$-2\mathrm{i}\omega_2 g^2\left[\left(\chi_{a,+}^{*-1}\chi_{b,+}^{*-1}\bar{\chi}_{b,+}^{*-1}-2\mathrm{i}\omega_2 g^2\right)(n_1+1)+\left(\chi_{a,+}^{-1}\chi_{b,+}^{-1}\bar{\chi}_{b,+}^{-1}-2\mathrm{i}\omega_2 g^2\right)n_1\right]\Bigg\}\ . \tag{S30}$$

For simplicity, we calculate the symmetrized power spectral density

$$\bar{S}_{xx}[\omega]=\frac{1}{2}(S_{xx}[\omega]+S_{xx}[-\omega])$$
$$=\frac{\hbar\gamma_1\left(n_1+\frac{1}{2}\right)}{2m\omega_1}\left(\left|\chi_{a,-}+2\mathrm{i}\omega_2 g^2\chi_{a,-}^2\chi_{b,-}\bar{\chi}_{b,-}\right|^2+\left|\chi_{a,+}-2\mathrm{i}\omega_2 g^2\chi_{a,+}^2\chi_{b,+}\bar{\chi}_{b,+}\right|^2\right)\ . \tag{S31}$$

This $\bar{S}_{xx}[\omega]$ can be separated into two parts $\bar{S}_{xx}[\omega]\triangleq\bar{S}_{xx}^{(+)}[\omega]+\bar{S}_{xx}^{(-)}[\omega]$, where

$$\bar{S}_{xx}^{(+)}[\omega]=\frac{\hbar\gamma_1\left(n_1+\frac{1}{2}\right)}{2m\omega_1}\left|\chi_{a,-}+2\mathrm{i}\omega_2 g^2\chi_{a,-}^2\chi_{b,-}\bar{\chi}_{b,-}\right|^2 \tag{S32}$$

contains intensity mainly in the positive frequency bands, and

$$\bar{S}_{xx}^{(-)}[\omega]=\frac{\hbar\gamma_1\left(n_1+\frac{1}{2}\right)}{2m\omega_1}\left|\chi_{a,+}-2\mathrm{i}\omega_2 g^2\chi_{a,+}^2\chi_{b,+}\bar{\chi}_{b,+}\right|^2 \tag{S33}$$

in the negative bands.

BACKGROUND INTENSITY

When measuring diffuse features in INS, proper assessment of the background intensity from the instrument, and the environment around the sample, is paramount. Part of the data correction includes measurements of the empty

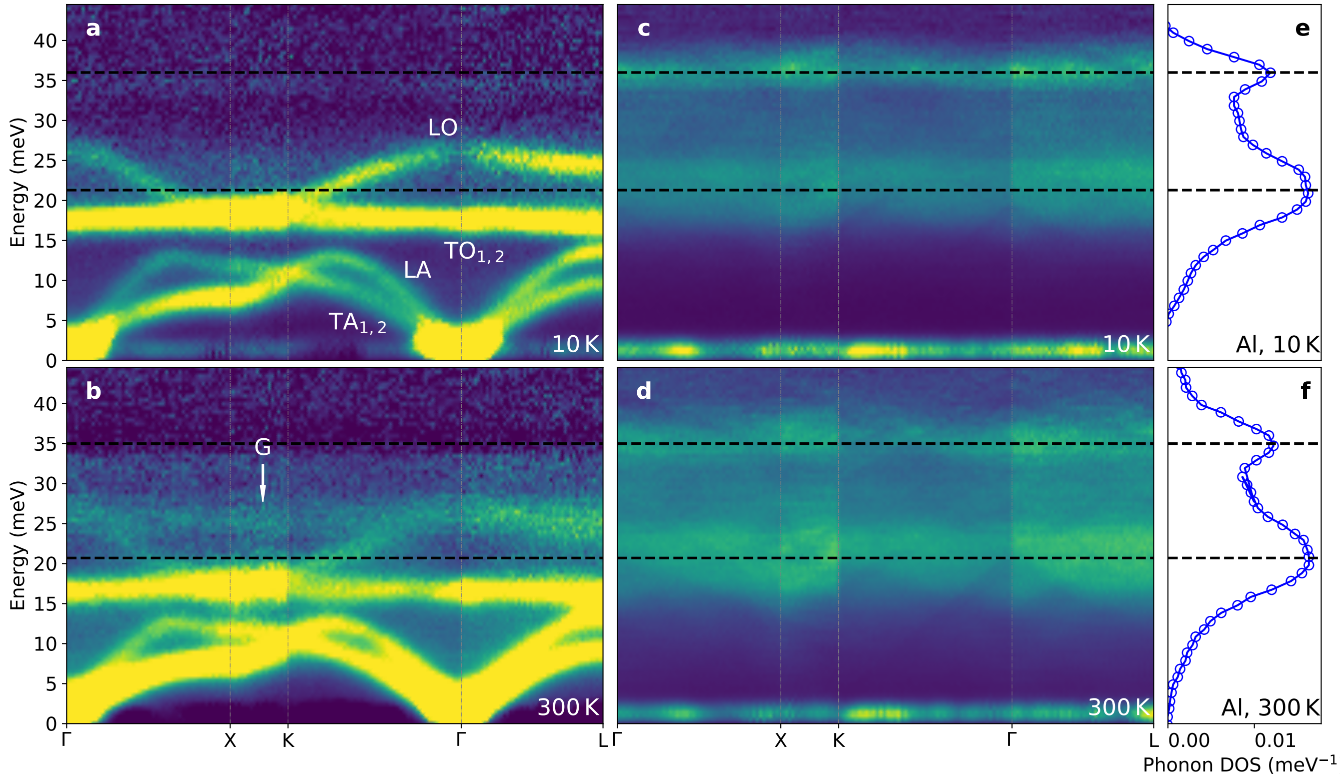

FIG. S1. **Information on background analysis. a-d,** 2D slices through the four-dimensional scattering function $S(\mathbf{Q}, \varepsilon)$, where $\varepsilon = \hbar\omega$, along high symmetry lines in the first Brillouin zone, measured at 10 K (**a, c**) and 300 K (**b, d**) respectively. **a-b** are the final results of single crystal NaBr and **c, d** are the background measurements of the empty aluminum can. Corresponding aluminum phonon DOS from previous measurements [2] are shown in **e** (10 K) and **f** (300 K). 'G' marks the intermodulation phonon sideband.

sample container under identical conditions. The empty can background, folded into the first Brillouin zone, is shown in Fig. S1c,d, and is compared with Fig. 1 in the manuscript. The background has two peaks centered at 20 and 35 meV (Fig. S1e,f), consistent with the phonon density of state (DOS) from polycrystalline aluminum at 300 K [2]. The new diffuse feature is at 25 meV, however, so it cannot be the residue of the sample container. We also confirmed that the diffuse feature cannot be formed by the excessive subtraction of the background – this gives a much wider peak spanning the energy range between 20-35 meV. Furthermore, the temperature dependence of the background follows that of the main dispersions in NaBr, but the diffuse features are far weaker than the main dispersions at 10 K, but modestly weaker at 300 K.

TEMPERATURE DEPENDENCE OF INTERMODULATION PHONON SIDEBANDS

The IPS spectra are much weaker at 10 K than at 300 K, owing to the temperature dependence of the Planck factors for phonon populations. Figure S2 shows how few one-phonon spectra (before renormalization) are excited at low temperature. This limits the number of the TA phonons within 7-9 meV that are available to participate the

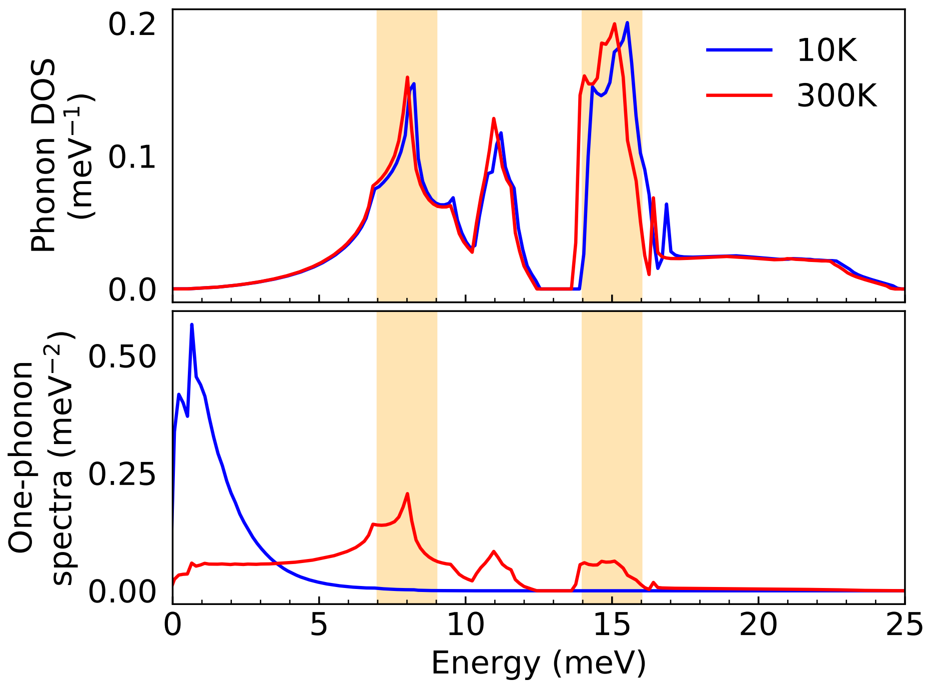

FIG. S2. **Calculated phonon DOS and one-phonon spectra before phonon self-energy corrections.** Phonons involved in the three-phonon processes for IPS feature are indicated by the shaded regions. The one-phonon spectra is given by $A_1(\epsilon) = \frac{g(\varepsilon)}{\varepsilon}\frac{1}{e^{\varepsilon/k_\mathrm{B}T}-1}$, where $g(\epsilon)$ is the phonon DOS.

three-phonon processes to generate the intermodulation sidebands.

* yshen@caltech.edu

† btf@caltech.edu

[1] J. Chan, T. M. Alegre, A. H. Safavi-Naeini, J. T. Hill, A. Krause, S. Gröblacher, M. Aspelmeyer, and O. Painter, Laser cooling of a nanomechanical oscillator into its quantum ground state, Nature **478**, 89 (2011).

[2] X. Tang, C. W. Li, and B. Fultz, Anharmonicity-induced phonon broadening in aluminum at high temperatures, Phys. Rev. B **82**, 184301 (2010).

TABLE S1. Fitting parameters.

Peak fitting function: $y = y_0 + \frac{2A}{\pi}\frac{w}{4(x-x_c)^2+w^2}$											
Panel in Fig. 5		a	b	c	d	e	f	g	h	i	j
q-point		[0, 0, 0]	[0, 0, 0.25]	[0, 0, 0.5]	[0, 0, 0.75]	[0, 0, 1]	[0, 0.75, 0.75]	[0, 0.5, 0.5]	[0, 0.25, 0.25]	[0.25, 0.25, 0.25]	[0.5, 0.5, 0.5]
Offset, y_0		0.0013(3)	-0.00001(6)	-0.0024(2)	-0.0015(2)	-0.0019(2)	-0.0008(2)	-0.0007(3)	-0.0037(5)	-0.0005(3)	-0.0008(3)
1st. peak	Center, x_1	16.58(7)	3.86(4)	6.05(2)	7.36(2)	7.73(3)	10.33(7)	8.48(7)	4.48(7)	6.09(12)	9.01(11)
	Width, w_1	2.8(3)	3.6(2)	3.57(11)	3.25(11)	3.35(11)	4.7(3)	3.9(3)	3.3(3)	2.5(4)	3.1(4)
	Area, A_1	0.038(4)	0.142(9)	0.086(3)	0.077(3)	0.088(3)	0.078(5)	0.045(5)	0.051(10)	0.040(9)	0.045(6)
	Height, H_1	0.010	0.025	0.013	0.014	0.015	0.010	0.007	0.006	0.010	0.009
2nd. peak	Center, x_2	26.3(3)	16.74(15)	11.45(10)	12.37(7)	11.92(7)	17.90(9)	12.18(8)	7.4(3)	9.1(2)	13.52(16)
	Width, w_2	3.8(15)	3.7(6)	4.6(4)	2.5(3)	2.3(3)	4.3(3)	2.8(3)	6.8(7)	4.2(7)	2.6(6)
	Area, A_2	0.012(5)	0.043(8)	0.033(3)	0.018(2)	0.019(2)	0.056(4)	0.022(3)	0.11(2)	0.060(12)	0.034(10)
	Height, H_2	0.002	0.007	0.005	0.005	0.005	0.008	0.005	0.010	0.009	0.008
3rd. peak	Center, x_3	-	25.9(6)	17.07(5)	17.40(5)	17.27(5)	26.3(3)	16.90(7)	16.74(6)	16.68(12)	16.40(19)
	Width, w_3	-	7(2)	3.6(2)	4.0(2)	4.8(2)	6.6(14)	4.2(3)	4.4(3)	3.2(4)	3.0(6)
	Area, A_3	-	0.030(14)	0.046(3)	0.063(3)	0.088(4)	0.033(7)	0.044(4)	0.049(4)	0.042(5)	0.040(10)
	Height, H_3	-	0.003	0.008	0.010	0.012	0.003	0.007	0.007	0.008	0.008
4th. peak	Center, x_4	-	-	24.8(2)	26.3(2)	26.4(2)	-	21.49(11)	25.72(14)	25.6(4)	25.8(5)
	Width, w_4	-	-	13.6(16)	9.1(11)	8.5(12)	-	2.0(5)	11.7(10)	9.5(19)	12(2)
	Area, A_4	-	-	0.102(14)	0.058(7)	0.052(7)	-	0.008(2)	0.12(2)	0.063(13)	0.096(19)
	Height, H_4	-	-	0.005	0.004	0.004	-	0.003	0.007	0.004	0.005
5th. peak	Center, x_5	-	-	-	-	-	-	25.7(3)	-	-	-
	Width, w_5	-	-	-	-	-	-	7.2(12)	-	-	-
	Area, A_5	-	-	-	-	-	-	0.038(8)	-	-	-
	Height, H_5	-	-	-	-	-	-	0.003	-	-	-